First evidence of polar mesosphere summer echoes observed by superdarn SANAE HF radar in Antarctica

Olakunle Ogunjobi*,Venkataraman Sivakumar and J. A. E. Stephenson

School of Chemistry and Physics, University of KwaZulu-Natal, Durban, South Africa
* **E–mail:** olakunle.ukzn@gmail.com, **Phone number:** +27 84824 2132

Abstract

Polar Mesosphere Summer Echoes (PMSE) have been the subject of much research over the last 3 decades. The proposed dependence of PMSE occurrence on extremely low polar mesosphere temperatures have resulted in numerous efforts to obtain convincing correlations. For the first time, we report the PMSE occurrence characteristics over SANAE IV (South African National Antarctic Expedition IV). A matching coincidence method allowing filtration of possible contaminating echoes is described and implemented for extraction of SuperDARN–PMSE during the 2005–2007 summers. In this method, measurements from Riometer and Super Dual Auroral Radar Network (SuperDARN) are fitted to obtain SuperDARN–PMSE occurrence probability rate. We establish that the seasonal and diurnal variations followed the known features of PMSE. The occurrence rate is found to be high in the summer months reaching ∼50% peak around the summer solstice. The PMSE occurrence on the day–to–day scale show predominantly diurnal variation, a broader maximum peak between 12–14 LT and distinct minimum of 22 LT. The use of quite day cosmic radio noise curves to filter ionospheric echoes from SuperDARN–PMSE detection does not change the SuperDARN–PMSE occurrence variations. Seasonal variations show a connection between the SuperDARN–PMSE occurrence rate and mesopause temperature. Seasonal and interannual variations of SuperDARN–PMSE correlate with mesospheric neutral winds. The SuperDARN–PMSE occurrence increased with the southward turning of meridional winds and zonal wind shear. The seasonal trend of both the meridional winds and zonal winds is repeated year–to–year. Analysis of the neutral wind variations indicates importance of gravity waves in SuperDARN–PMSE generation.

Keywords: PMSE; SANAE IV; SuperDARN radar; Neutral winds; MLT Temperatures

1 Introduction

It is generally accepted that, during polar summer time, both charged ice aerosol particles and mesospheric neutral air turbulence play a significant role in the creation of electron number density (Rapp and Lübken, 2004). The interactions of the charged ice particle and turbulence results in strong radar backscatter echoes in polar mesopause (90–100 km) regions. These echoes are refereed as polar mesosphere summer echoes (PMSE). The PMSE are closely linked to visible ice particles below 90 km altitude, known as noctilucent clouds (NLC) (Cho, 1997; Rapp and Lübken, 2004). The phenomena of NLC and PMSE arise from the formation of ice particles in the low temperatures of the polar summer mesopause. It has been suggested, nevertheless, that NLC and PMSE are comparatively different in their occurrence. NLC indicates the presence of thin water–ice particles, formed at low summer mesopause temperature, between 120 to 150 K (Hervig et al., 2009). Whereas, an additional precondition for PMSE occurrence is the presence of charged ice particles on the scale of Bragg's wavelength. It is broadly noticed by the earlier researchers that the occurrence of PMSE is due the combination of atmospheric turbulence produced by gravity waves and electrically charged ice particles within the mesosphere (see, Rapp and Lübken, 2004). Therefore, PMSE partly represent mesospheric features and to address the better understanding of neutral atmosphere and role of dynamics. Also, PMSE observations with radar have the advantage of being continuous, unlike NLC which depends on the observer and weather conditions (Rapp and Lübken, 2004). In recent times, observations of PMSE have been found to support the understanding of temperature modification between the Arctic and Antarctic mesopause regions (Huaman and B., 1999). Intuitively, neutral wind circulation induced by gravity waves, is expected to result in a decrease temperature at mesospheric altitude, where ice particles can be formed from the water vapor. However, several characteristics of PMSE indicate that polar mesospheric temperature may be highly dynamic.

Over the last 3 decades, coherent VHF radars have been found to be a useful tool in studying PMSE dynamics mostly in the Arctic regions (Ecklund and Balsley, 1981; Palmer et al., 1996; Hoffmann et al., 1999; Rapp and Lübken, 2004). Notwithstanding, the characteristics of PMSE and the occurrence rates in the Antarctic regions are not yet to be completely understood. There has been a notable absence of sufficient suitable measurements in Southern hemisphere. Nevertheless, the few coherent VHF observations from Antarctic indicate irregular distribution in PMSE due to complex mesospheric thermal phenomena in both hemispheres. These complex events range from periodic and episodic to perturbations to those on a global scale. Nonetheless, studies have observed PMSE at VHF frequency ranges in correlation and anti–correlation to temperature, neutral winds, particle precipitation, cosmic noise absorption and gravity waves (Cho et al., 1992; Kirkwood, 1993; Röttger, 1994; Hoffmann et al., 1999; Klostermeyer, 1999; Liu et al., 2002; Klekociuk et al., 2008). There are ongoing efforts to complement the VHF observation of PMSE with that of coherent HF super Dual Auroral Radar Network (SuperDARN) e.g (Hosokawa and Ogawa, 2004; Ogawa et al., 2004; Hosokawa et al., 2005; Liu et al., 2013). Hosokawa et al. (2005), for example, developed an algorithm for extracting PMSE from SuperDARN Syowa HF radar in Antarctic and Iceland in Arctic. The algorithm was employed with a careful consideration of other overlapping echoes such as meteor trails, and sporadic E–region echoes in the range of PMSE. The result of Hosokawa et al. (2005) shows weaker interhemispheric asymmetry in PMSE occurrence than earlier predictions based on VHF radar observations. A similar algorithm was also employed by Liu et al. (2013) for extracting PMSE from SuperDARN Zhongshan HF radar (69.41°S, 76.41°E). In order to avoid contamination from ionospheric echoes Liu et al. (2013) extracted PMSE from SuperDARN when $Kp \leq 1$. It was suggested from their observation that the auroral particle precipitation might be a major contributor to the PMSE occurrence. During maximum solar activity, energetic particle precipitation and levels of Extreme ultraviolent (EUV) radiation could be high. It is however expected that solar quiet time electrodynamics of the Mesosphere and Lower Thermosphere (MLT) region will be driven mainly by gravity waves, tides and planetary waves propagating upward from their source regions in the lower atmosphere (Richardson et al., 2001). Here, PMSE observations with SuperDARN SANAE IV radar (71.68°S, 2.85°W), herein refer to as SuperDARN–PMSE, during the recent prolonged solar minimum add valuable insights in this field. Furthermore, understanding the dynamics of the Southern hemisphere PMSE variability requires evidence and characteristics from different locations and during different seasons (Morris et al., 2004; Jarvis et al., 2005).

This paper presents first time observations of PMSE by a SuperDARN HF radar at SANAE. The summer periods of year 2005–2007 solar minimum were analysed. Several factors (ionospheric irregularities aspect conditions, initial conditions and QDC) were taken into account to ensure that echoes were valid PMSE observations. Seasonal, diurnal and interannual variations were determined. Furthermore, we investigated the relationship between seasonal variations of PMSE occurrence rate and mesospheric neutral winds and furthermore analyse the effects of changes in monthly– and seasonal–mean winds associated with the begin of the SuperDARN–PMSE season. Finally, we briefly discussed possible temperature changes in relation to neutral winds during the occurrence of SuperDARN–PMSE.

2 Instrumentation and data analysis

Data from the SuperDARN SANAE IV radar is employed in this study. The radar uses the frequency band between 8 and 20 MHz. The antenna array consists of 16 antennae, which are operated as a phased array having 170° bore–site. SANAE IV radar is technically and operationally similar to other 32 SuperDARN radars located at polar and mid latitudes. The SuperDARN radars at different locations use the same scanning parameters for 50% of the entire instrument operational time (Greenwald et al., 1995; Hosokawa et al., 2005). The remaining

50% time, individual radar usage can be discretionary thus the parameters can be changed. The radar data used in the present analysis were obtained during periods of common time operation. In common time operation, the SuperDARN radar beam is sequentially scanned from beam 0 to beam 15 across its 75 range gates with a step in azimuth of 3.33°, a scan repeat time at for 2 minutes, a range resolution of 45 km, and a peak power of about 10 kW. The beams to have maximum sensitivity at elevation angles of 15°–35° to allow backscatter echo detection. The return echoes for each beam are integrated over 3 or 7 s. The field of view (FOV) of SANAE IV radar in geographic and geomagnetic coordinates is presented in Figure 1. The FOV shows that SuperDARN SANAE IV radar is located at the sub auroral location suitable for observations of HF backscatters within the Antarctic region. The target of SuperDARN rdars re coherent. They include field aligned irregularities in the ionospheric E and F region, and of importance to this work, meteor trail, sporadic E regions echo and PMSE. The oblique sounding technique of SuperDARN is such that it can detect these backscatters simultaneously within the near range gates. The backscatter delays at the nearest range gate (0 gate) is set to 1200 μs pulse length, which is equivalent to 180 km. The subsequent pulse length is set to 300 μs, equivalent to a gate length of 45 km. In this study, the near range gate is taken from 0 to 1 which corresponds to a distance of 180–225 km. The near range gates correspond to mesospheric altitudes. In order to isolate PMSE from other contaminating echoes, a systematic approach is required (Hosokawa et al., 2005). Only PMSE, according to Hosokawa et al. (2005), has been judged to be present in the near gate if both spectral width and Doppler velocity measurements are less than 50 m/s, and power is greater than 6 dB. However, this algorithm does not necessarily preclude contaminations from ionospheric E–region echoes.

Figure 2 depicts the typical instances of these three forms of backscatter features. In Figure 2 (left panel), from top to bottom panels are range versus time plots of backscatter power, Doppler velocity and spectral width of echoes observed in which only beam 12 is displayed on 21 December 2005. During the period of summer solstice, backscatters return echoes were found to be higher compared to 21 April 2005 in Figure 2 (right panel). It is a probable that polar mesospheric summer echoes which might have contributed to the high rate of backscatters detected in the summer solstice. Discrimination of the PMSE from contaminated returns, such as ionospheric E–region echoes, needs other procedures which impose further restrictive conditions. The E–region irregularities, in particular is known be aspect sensitive(Liu et al., 2013).

In order to eliminate the effects of E–region echoes or the background cosmic noise from PMSE detection, we follow two procedures. First, the range–time plot from the VirginiaTech website `http://vt.superdarn.org` was inspected for aspect angle conditions for the radar near ranges. We found that the aspect angle conditions could not have been met at gate 0–1. All the radar beams (0–15) were then inspected to ensure that at the radar near range, the aspect angle condition for E–region irregularity is not satisfied. Second, we use the ionospheric absorption measurements from the ground based riometer located at SANAE IV. E–region irregularities have been correlated with geomagnetic disturbances resulting in aurora (Greenwald et al., 1995; Zhang et al., 2013; Liu et al., 2013). On the other hand, the visible aurora is an effect of precipitating energetic particles interacting with the Earth's magnetic field. The interactions can, perhaps, create steep electron density gradients and by extension cause cosmic radio noise at mesopause region over SANAE IV e.g (Ogunjobi et al., 2014; Wu et al., 2013). Riometers respond to the integrated absorption of cosmic ray noise through the ionosphere (Wilson and Stoker, 2002; Hargreaves and Friedrich, 2003) usually around 90 km altitude. The data from riometer may permit us to indirectly eliminate and thus allow us to avoid ionospheric echoes produced during the energetic particle precipitation into the atmosphere. In order to consider absorption signal caused by the precipitation during geomagnetic storm, we obtained a quiet day curve (QDC) for SANAE IV. By performing the QDC, a threshold of 1 dB was taken. In this work, only the events that fall below the QDC were retained as candidate SuperDARN–PMSE.

Additionally, SuperDARN observation of meteor trails at 94 km is associated with drift in neutral wind velocities which is useful in studying the trends of meridional and zonal circulations. Although SuperDARN radar is not specifically planned for wind observation, but it can be used to track neutral wind variation at mesopause altitude. A detailed description of tracking, neutral winds using SuperDARN radar can be found elsewhere (Hussey et al., 2000; Chisham et al., 2007). It should be noted bowever, that winds are altitude dependent and thus meteor radar observation of neutral winds can only be relative. This caveat in using wind measurements from meteor radar has been noted by Yukimatu and Tsutumi (2002, 2003). Recent updates on SuperDARN operations can also be found in Lester (2013).

In order to examine any potential connection between SuperDARN–PMSE and mesospheric temperature we obtained the average of TIMED/SABER (Thermosphere Ionosphere Mesosphere Energetic and Dynamics / Sounding of the Atmosphere using Broadband Emission Radiometry) vertical temperature. Details on how SABER is retrieved will be discussed later. Anyway, the TIMED satellite was launched on 7 December 2001. It is nadir–pointing and has 625 km circular polar orbit at 74.1° inclination and has a period of 102 minute. By step scanning the atmosphere limb, SABER, which is one of the four instruments on–board the TIMED satellite, measures the height profile of neutral temperature. In this study, the vertical temperature measurements in the vicinity of SANAE IV were obtained. It should be noted that in this study, winter refers to April–September and summer in October–March.

3 Results and discussion

3.1 Characteristics of SuperDARN–PMSE

SuperDARN–PMSEs are judged present if certain conditions are met. Clean SuperDARN–PMSE events require backscatter power above 6 dB and, Doppler velocity as well as spectral width below 50 m/s. We shall refer to these conditions as initial SuperDARN–PMSE conditions. To eliminate possible enhanced cosmic noise, initial conditions were further subjected to background noise test using QDC. On the other hand, it has been known that ionospheric irregularity has aspect angle sensitivity. Thus, we ascertained that the aspect angle conditions for ionospheric irregularity was not satisfied at the radar near range gate. The occurrence rate was computed from the near range and then calculated in 10 minute intervals for the period under study.

Figure 3 shows the SuperDARN–PMSE probability of occurrence, during the Antarctic summer seasons of 2005/2006. During the summer months we have observed an increased number of PMSE occurrence. The SuperDARN–PMSE occurrence starts to to rise around November 2005, thereafter it has increased steadily upto December 2005, while having the highest number of occurrence during the end of January 2006. The probability rate of SuperDARN–PMSE occurrence peaks near the summer solstice at 50% for SANAE IV. These statistical results are similar to previous studies in VHF frequencies despite the differences in location, time and experimental setup of the radars. The seasonal variation is also similar to previous observations from HF radar. Using SuperDARN HF radar, Hosokawa et al. (2005) found that the PMSE occurrence shows a sudden increase in the beginning of the summer season, maximises days after the summer solstice, and a gradual decay to the end of January. This is in good agreement with PMSE observation by Hoffmann et al. (1999). It should be noted that, the determination of near range contamination depends on the specific location and the radar characteristics which might vary slightly from one radar to another. For instance,Liu et al. (2013) found that at Zhongshan HF radar station, there was a maximum peak near local midnight and secondary peak few hours after the local noon. They attributed this to role of precipitating energetic particles. They also showed that the aspect angle condition for ionospheric echoes could not have been satisfied at gate 0–2. Although we have seen similar trend for local noon but we can not find tendency for the midnight peak. This could be due to Zhongshan station being directly under the auroral oval. Solar wind can energise the radiation belt particles with enough energy to spiral into the atmosphere and produce aurora. This aurora precipitation is confined to a zone known as the auroral oval. It should be noted that SANAE IV is not directly under, but somewhat equatorward of, the auroral oval as Zhongshan. We prefer to be cautious with our conclusion regarding diurnal SuperDARN–PMSe occurrence rate here; because the atmospheric features such as planetary waves and tides may cause the PMSE diurnal trend to take longer time to be observable. Also, this observation is for a particular summer season thereby far from conclusive for SANAE IV PMSE.

Referable to the above limitation in making conclusion regarding the diurnal trends, we studied the following summer for any significant inter annual variation over our region of interest. Figure 4 presents SuperDARN–PMSE occurrence for 2006/2007 over SANAE IV. There is no significant difference of inter annual SuperDARN–PMSE variations. The probabilities of occurrence remains enhanced reaching a maximum peak of 50% for SANAE IV around the same summer solstice. The observed time for preceding summer season (Figure 3) reveals similar trend. The inter–annual similarity in the occurrence probability rate over SANAE IV could be due to a persistent situation during the declining phase of solar cycle. Since the events for SANAE IV quite times was extracted, the QDC employed might have probably filtered any contamination capable of inducing significant annual variability.

The evidence of insignificant inter annual variation, allow us to combine diurnal SuperDARN–PMSE rates profile for both summers. The echoes rates were combined in a vector addition to yield hourly variation. In this method, for each hour of the day, a mean was taken of all the values for that hour over the summer seasons. This yielded a combined mean diurnal rate for both 2005/2006 and 2006/2007 summer months. In Figure 5, the diurnal variations in the SuperDARN–PMSE occurrence rate is characterised by the highest peaks around 12 LT and minimal near 22 LT. The broad maximum obtained at 11–13 LT is also similar to previous VHF and HF observations in several high latitude locations. Similar to other HF radar study at Syowa, Hosokawa et al. (2005) observed diurnal maximum PMSE occurrence around 13 LT and minimum occurrence been 1 hour time lag compared to our observation. The similar diurnal trend was previously observed by Hoffmann et al. (1999) with a clear maximum at 13–14 LT and a pronounced minimum at 19–21 LT. However, using SuperDARN radar, Liu et al. (2013) noted a semidiurnal variation of PMSE occurrence at Zhongshan station. Their observed maximum PMSE occurrence was observed near 0 LT and a secondary maximum near 13 LT while a distinct minimum was near 19 LT. Balsley et al. (1983); Morrison et al. (2007); Latteck et al. (2008) had earlier reported that the occurrence of PMSE has a broad maximum at 1–2 h after the local noon and that the secondary peak usually appears around the local midnight. In this study, we did not observe such semidiurnal characteristics. Over the past few years, PMSE observations have shown maximal and minimal with different instruments used to examine it. Some discrepancies (usually $\pm$ 2 hr) exist in the determination of the temporal positions of maxima and minima. This can be due to sidereal time of the day, which differs from one location to another. It may also be linked to the aspect angle sensitivity of E–region echoes which may differ in the case of HF radars. In the case of VHF radars, the threshold of volume reflectivity and signal to noise ratio may result in some temporal discrepancies (Smirnova et al., 2010). Although the existence of the diurnal and semidiurnal variations has been widely reported, the causative mechanism is yet to be completely understood. In this study, we observed broader maximum of SuperDARN–PMSE at noon and a distinct mimimum at midnight. While this generally agrees with the previous observations, the discrepancies in terms of semidiurnal variations could be that PMSE occurrence could depend on numerous factors including: electron density (Kirkwood, 1993), 3hr–shifted meridional winds (Hoffmann et al., 1999), temperature (Klostermeyer, 1999), planetary waves Klekociuk et al. (2008) and energetic particle precipitation (Liu et al., 2013) at the same heights of PMSE.

All these phenomena, in turn, depend on the longitudinal location of the observations. Liu et al. (2013), for example, argued that since Zhongshan Station lies under the auroral oval near 0 LT and around 13 LT, the auroral particle precipitation influence the PMSE occurrence. The auroral particle influence of Zhongshan PMSE could have resulted in the special diurnal variation with two distinct PMSE peaks despite the fact the Liu et al. (2013) used Kp index as proxy to avoid ionospheric echoes. In this study, we use cosmic radio noise absorption. There is an important difference between the indices and the noise absorption approach. The Kp index is valued based on global geomagnetic field measurements and thus depends on the electron density above 100 km; whereas cosmic noise absorption is determined by height integrated electron density below 100 km (Smirnova et al., 2010). Here, we found that the SuperDARN–PMSE occurrence probability does not have special diurnal variation showing two distinct peaks; rather, we observed only broader maximum at noon times and distinct minimum at midnight. The QDC employed together with the initial SuperDARN–PMSE conditions could have averaged out precipitating particles influence at SANAE IV. So, we can not, at this point, conclusively rule out the possibility of semidiurnal variability over SANAE IV. The way forward would require examination of the parameters used for the initial conditions. The trend of these parameters, without considering QDC or ionization, might be more correct method to reveal any background effects on SuperDARN–PMSE at SANAE IV.

3.2 Velocity, width and power effect

Figure 6 shows the monthly variation of mean Doppler velocity, spectral width and power. These aforementioned parameters are competing factors that may influence the form of the SuperDARN–PMSE. Since the average expected from near the range gate depends on the intensity on returns, these parameter trends is compared with SuperDARN–PMSE rates. In Figure 6 (a), we observe the high level velocity during the winter (around late March) and gradual decrease towards the summer (late November) when PMSE occurrence was increasing. The echoes Spectral widths in the winter months are larger than those in the summer months average of 200 m/s as shown in Figure 6 b). There are two broader maximum regions: first broader maximum is seen from July to September and second from April to June. The spectral widths generally decrease in the summer months when a significant PMSE occurrence was observed. In Figure 6 (c), the monthly variations of average power is similar to that of PMSE frequency of occurrence. Solar irradiation is usually high in the summer months, thus, low radar power is expected. The increasing rates of PMSE at lower power is attenuated towards the beginning of winter by larger values spectral width. This observation agrees with the SuperDARN–PMSE statistics shown in Figure 3 and Figure 4. The highest distribution is shifted towards the summer solstice, suggesting that in the majority of cases, the PMSE follows the initial conditions. Therefore there is a similar PMSE trends with the Doppler velocity, spectral width and power. This might mean that the mechanism responsible for SuperDARN–PMSE variations reflected by the initial conditions, holds true. This is in agreement with HF–VHF radar observations at Syowa in Antarctica by Ogawa et al. (2004). The diurnal curves for velocity, width and power (not shown) also reveal similar trends as the day–to–day SuperDARN–PMSE variation.

This analysis also provides an indirect confirmation on the relationship between cosmic radio noise absorption and SuperDARN–PMSE. The echoes distribution shown in Figure 7, with a 50% occurrence rate, was extracted without consideration to QDC (i.e PMSE extracted based on only velocity, width and power). Compared with Figure 3 and Figure 4 when QDC was employed shows that SuperDARN–PMSE has no significant correlation with cosmic noise absorption. This means that the aspect angle conditions not being met at near range, is indeed useful in isolating ionospheric echoes(Liu et al., 2013). This is in agreement with previous work, Barabash et al. (2002) did not find significant correlation between PMSE variations and cosmic noise absorption. In contrast, Morris et al. (2005) found a very weak correlation of PMSE and cosmic noise absorption. This may be attributed to long HF radar wavelength compare to VHF radar wavelengths. At HF, one is observing icy dust particle charging whereas at VHF one is observing electron diffusion, which requires strong density gradient and by extension peak cosmic absorption. With this observation, we suggest that long time study, i.e a complete solar cycle, of SuperDARN–PMSE over SANAE IV radar would confirm this statistical result. Other factors can also induce significant influence on PMSE if varies over many years, for example, the neutral wind forcing. Since SANAE IV is at sub–auroral location, we may expect neutrals to dominate. Though domination of neutral circulation at aurora D–region may be expected, the trend in relation to SuperDARN–PMSE season may be significant. Therefore, analysis of variations in both temperature and neutral winds would be considered.

3.3 Temperature and neutral winds effect

To investigate a possible connection between SuperDARN–PMSE and mesospheric temperature we present the average of SABER vertical temperature during the SuperDARN–PMSE seasons is presented in Figure 8. SABER is measuring CO_2 15 μm limb emission which can be used to estimate the neutral temperatures up to approximately 130 km. In order to maintain a certain temperature in the instrument, SABER obtains profiles from 83°S to 52°N during its south–looking mode and at every 60 days the look direction switches to an analogous North–looking mode. Here, SABER temperature measurements are during its south–looking mode. The data were then detected for the vicinity of SANAE IV (i.e, 71 +/− 4° and 2 +/− 10° latitude and longitude respectively). We combined temperature measurements for the year 2005/2006 and year 2006/2007 SuperDARN–PMSE season. It should be noted that there was no SABER temperature data for the February months as SABER was in North looking mode. From the figure (Figure 8) it can be seen that, close to the solstice, there is a lowering of mesopause temperature till January (i.e., 30 days after the summer solstice), whereas in March the vertical temperature starts to increase. Comparing with SuperDARN–PMSE seasonal distribution in Figure 7, which is very similar, leads us to inspect a linkage between the occurrence rate and temperature. Prior to the summer solstice in November, the temperature is found to be approximately 149 K around mesopause region tied to around 10% superDARN–PMSE occurrence rate. In December, temperature is observed have decreased value reaching about 134 K while SuperDARN–PMSE rate also increased significantly (around 50%). Unfortunately, temperature measurements was not available in our region of interest in February when the SuperDARN–PMSE rate started decreasing. Nevertheless, temperature for March provides what should be anticipated as it increases up to 204 K with an occurrence rate being much lower than the pre–summer solstice. In order to make a quantitative analysis over the potential correlation between the aforementioned parameters, we have obtained neutral wind measurements from SuperDARN SANAE IV radar.

SuperDARN radars were basically designed to detect ionospheric backscatter and to study the dynamics of the high–latitude ionosphere Greenwald et al. (1995). However, SuperDARN radars also detect echoes from other sources such as from meteor echoes. The radar detection of meteor echoes around 94 km altitude is associated with velocity drift, which can be used to study neutral winds variation. Observation of neutral winds with radar may not be a perfect proxy as pointed out by Yukimatu and Tsutumi (2002, 2003) as wind velocity is altitude dependent. However, SuperDARN radar may track the neutral wind within 90–94 km, thus provide a good information regarding the trend of meridional and zonal winds in relation to SuperDARN–PMSE observed.

Theoretical explanations of how the gravity wave drives meridional circulation from the winter to summer mesosopause is provided by Andrews et al. (1987). This driven circulation results in extremely low temperature at the summer mesopause–a condition necessary for PMSE occurrence. In order to test this theoretical assumption by Andrews et al. (1987) in relation with SuperDARN–PMSE observation, we investigated the change of meridional and zonal wind components. Further, we want to confirm if our previous analysis implies that the mechanism responsible for SuperDARN–PMSE variations is steady over the long term. Here we obtained radar measurements of neutral winds from the year 2002–2007. Figure 9 (top panel and bottom) presents contours of all the available monthly–mean winds. The gap in the Figures which covers the early part of 2007 results from data gaps in SANAE IV superDARN radar. This Figure provides a clear indication of how the monthly–mean winds vary from year to year. Since the data analysis is based on monthly averages, we might ignore the short periodic waves. In both meridional wind (Figure 9 top) and zonal wind (Figure 9 bottom) observed over SANAE IV, a seasonal pattern that repeats from year–to–year is evident, at least in summer. The most conspicuous feature is a period of strong equatorward (negative) meridional flow during the summer while the zonal wind shear became more poleward. Comparing with PMSE statistics shows that the SuperDARN–PMSE has a higher probability of occurrence with southward meridional wind and Eastward flow of zonal winds.

The knowledge of variations in meridional and zonal winds in SuperDARN–PMSE season in relation to mesopause temperature is important. Understanding the temperature relation requires the understanding of effects of tropospheric features in the mesopause. It is known that in the troposphere, the gravity waves can be excited by the current of air over mountains, thunderstorms, volcanic eruptions and earthquakes. This tropospheric gravity waves can propagate eastward or westward to the upper region of the atmosphere. Due to the presence of summer stratospheric westward (negative) winds, the eastward propagating gravity waves mode can arrived at the summer mesosphere, where they break (Lindzen, 1981; Offermann, 1985). Conversely, the westward propagating gravity wave mode, will reach the mesosphere in winter. The gravity waves breaking and the resulting momentum energy deposition to the mesopause will decelerates the zonal wind, and by thermal wind balances change the meridional temperature field (Lindzen, 1981; Schunk and Nagy, 2000). This will induce meridional circulation characterised by upwelling of the air mass at the summer polar mesopause. The upward lifting of the air mass causes its volume to expands adiabatically on the expense of internal energy of the parcel thereby temperature decrease (for example, Andrews et al., 1987). The equatorward wind observed in the summer (Figure 9 top) might have transported the cold air while the summer poleward wind in Figure 9 bottom may be associated with the warm air. In other words, the resulting the temperature decrease will be maintained throughout the summer mesopause by residual flow, aided by upwelling of the air mass and zonal–mean meridional flow. Generally, the equatorward flows of meridional circulations will induce cold air during summers. The cold air in turn is essential to ice particles which are formed from the water vapor–a condition that is partly required for PMSE occurrence. This correlates well with the generally accepted hypothesis on conditions necessary for PMSE generation. Comparing the observed neutral wind trends, it could also be affirmed that SuperDARN–PMSE occurrence rate over SANAE IV is stable and with no interannual variability. Since the trend of summer meridional winds are stable, it could infers that SuperDARN–PMSE has little significant inter annual variations. In a separate studies over Davis in Antarctica, Morrison et al. (2007); Morris et al. (2009) found changes in modulation of the PMSE in connection with meridional wind and the temperature structure of the mesopause region. In contrast, PMSE study at Andenes (Zeller et al., 2009) shows anti–correlation with temperature during the PMSE season in 2002. At that season, the mesospheric temperature over Andenes was anomalously high and close to the water vapor frost point. The implication is that PMSE occurrence might truly be more strongly influenced by other factors, such as planetary waves. However, there is yet to be adequate temperature measurements at SANAE IV and also temperature model parameters are somewhat subject to ambiguity at sub–auroral location. At aurora location, conductivity is not certain, electric field is dynamical, the linear coefficient between heating and cooling becomes less realistic. Also, the polar mesosphere and lower thermosphere (MLT) is too low for a total probe using in situ satellites thus measurements can only be estimate. A ground based LIDAR (Light Detection and Ranging) observation of temperature may provide a unique opportunity to fully study thermal responses including charged ice aerosol particles over SANAE IV. This will complement the present SuperDARN–PMSE observation in relation to polar mesopause temperature.

4 Conclusions

We have observed, for the first time, PMSE at near ranges of the SuperDARN SANAE IV radar. The observation used in this analysis were made during the 2005–2007 PMSE seasons. This period enable us to examine several characteristics of SuperDARN–PMSE during the recent solar minimum. After comparing the SuperDARN–PMSE occurrence with atmospheric features such as cosmic radio noise, winds and temperature, we come into the following conclusions.

- The SuperDARN–PMSE seasonal rate is enhanced at the beginning of December summer, remains at the highest level until several days after summer solstice and then gradually decreases towards the end of February.
- No interannual variation is seen in in the SuperDARN–PMSE occurrence probability rates, the maximum rate is 50% for different years.
- The SuperDARN–PMSE occurrence on the day–to–day scale show predominantly diurnal variation, a broader maximum peak between 12–14 LT and distinct minimum of 21 LT.
- The use of quite day curves to filter ionospheric echoes from SuperDARN–PMSE detection does not change the SuperDARN–PMSE occurrence variations hence it is not contaminated by cosmic noise absorption.
- The seasonal variations of SuperDARN–PMSE are found to correlate with mesopause temperature. The occurrence rate increases with the lowering of neutral temperature.
- The beginning of the SuperDARN–PMSE enhancement is associated with southward meridional winds and zonal wind shear.
- The seasonal trend of both the meridional winds and zonal winds is very stable from year–to–year hence the SuperDARN–PMSE variabilities are reproduced year–by–year. Gravity waves which drives meridional winds, might be a major contributor to SuperDARN–PMSE generation.

Acknowledgements The authors express thanks for the support of South Africa National Antarctic Program (SANAP) and logistics of South Africa National Space Agency (SANSA) in providing SANAEIV riometer data. SANAP, SANSA and HF radar group, University of KwaZulu–Natal, SA support the SANAE IV HF radar. The SuperDARN radar wind data is provided by British Antarctic Survey, UK, at http://psddb.nerc–bas.ac.uk. And the authors also express thanks to TAOs anonymous reviewers for their valuable comments and suggestions. Research is supported by SANSA.

References

Andrews, D., Holton, J., Leovy, C., 1987. Middle Atmospheric Dynamics. Academic Press, New York and London.

Balsley, B., Ecklund, W., Fritts, D., 1983. Mesospheric radar echoes at Poker Flat, Alaska: evidence for seasonally dependent generation mechanisms. Radio Science 18, 1053–1058.

Barabash, V., Chilson, P., Kirkwood, S., 2002. Are variations in PMSE intensity affected by energetic particle precipitation? . Annales Geophysicae 20, 539–545.

Chisham, G., Lester, M., Milan, S.E., Freeman, M.P., et al., 2007. A decade of the super dual auroral radar network (superdarn): scientific achievements, new techniques and future directions. Survey in Geophysics 28, 33–109.

Cho, J., Kelley, M., Heinselman, C.J., 1992. Enhancement of Thomson scatter by charged aerosols in the polar mesosphere: measurements with a 1.29 GHz radar. Geophysical Research Letters 19, 1097–1100.

Cho, J.Y.N., 1997. An updated review of polar mesosphere summer echoes' observation, theory, and their relationship. Journal of Geophysical Research 102 (D2), 2001–2020.

Ecklund, W., Balsley, B., 1981. Long–term observations of the Arctic mesosphere with the MST radar at Poker Flat, Alaska. Journal of Geophysical Research 86, 7777–7780.

Greenwald, R.A., Baker, K.B., Dudeney, J.R., Pinnock, M., Jones, T.B., Thomas, E.C., Villain, J.P., Cerister, J., Senior, C., Hanuise, C., et al., 1995. DARN/SuperDARN. Space Science Review 71, 761–796.

Hargreaves, J.K., Friedrich, M., 2003. The estimation of D-region electron densities from riometer data. Annales Geophysicae 21, 603.

Hervig, M.E., Gordley, L.L., Russell III, J.M., Bailey, S.M., 2009. SOFIE PMC observations during the northern summer of 2007. Journal of Solar–Terestrial Physics 71, 331–339.

Hoffmann, P., Singer, W., Bremer, J., 1999. Mean seasonal and diurnal variations of PMSE and winds from 4 years of radar observations at ALOMAR. Geophysical Research Letters 26, 1525–1528.

Hosokawa, K.T., Ogawa, N.F., 2004. Statistics of Antarctic mesospheric echoes observed with the SuperDARN Syowa radar. Geophysical Research Letters 31, L02106.

Hosokawa, K.T., Ogawa, N.F., Arnold, M., Lester, N.S., and, A.S.Y., 2005. Extraction of polar mesosphere summer echoes from SuperDARN data. Geophysical Research Letters 32, L12801.

Huaman, M.M., B., B.B., 1999. Differences in near–mesopause summer winds, temperatures, and water vapour at northern and southern latitudes as possible causal factors for inter–hemispheric PMSE differences. Geophysical Research Letters 26, 1529–1532.

Hussey, G.C., Meek, C.E., André, D., Manson, A.H., Sofko, G.J., 2000. A comparison of Northern Hemisphere winds using SuperDARN meteor trail and MF radar wind measurement . Journal of Geophysical Research 105, 18053–18066.

Jarvis, M.J., Clilverd, M.A., Rose, M.C., Rodwell, S., 2005. Polar mesosphere summer echoes (PMSE) at Halley (76S, 27W). Geophysical Research Letters 32, L06816.

Kirkwood, S., 1993. Modeling the undisturbed high-latitude E region. Advances in Space Research 13, 3101–3104.

Klekociuk, A., Morris, R., Innis, J., 2008. First Southern Hemisphere common volume measurements of PMC and PMSE. Geophysical Research Letters 35, L24804.

Klostermeyer, J., 1999. On the diurnal variation of polar mesosphere summer echoes. Geophysical Research Letters 26, 3301–3304.

Latteck, R., Singer, W., Morris, R., Hocking, W., Murphy, D., Holdsworth, D., Swarnalingam, N., 2008. Similarities and differences in polar mesosphere summer echoes observed in the Arctic and Antarctica. Annales Geophysicae 26, 2795.

Lester, M., 2013. The Super Dual Auroral Radar Network (SuperDARN): An overview of its development and science. Advances in polar science 24, 1–11.

Lindzen, R.S., 1981. Turbulence and stress owing to gravity wave and tidal breakdown. Journal of Geophysical Research 86, 97079714.

Liu, E.X., Hu, H.Q., Hosokawa, K., Liu, R.Y., Wu, Z.S., Xing, Z.Y., 2013. First observations of polar mesosphere summer echoes by SuperDARN Zhongshan radar. Journal of Atmospheric and Solar–Terrestrial Physics 104, 39–44.

Liu, J.Y., Pan, C.J., Lee, C.C., 2002. VHF radar and MF/HF dynasonde observations during polar mesosphere summer echoes conditions at EISCAT. Earth Planets Space 54, 691–698.

Morris, R., Holdsworth, D., Klekociuk, A., Latteck, R., Murphy, D., Singer, W., 2009. Inner-hemispheric asymmetry in polar mesosphere summer echoes and temperature 69 latitude. Journal of Atmospheric and Solar-Terrestrial Physics 71, 464–469.

Morris, R., Terkildsen, M., Holdsworth, D., Hyde, M., 2005. Is there a causal relationship between cosmic noise absorption and PMSE? . Geophysical Research Letters 32, L24809.

Morris, R.J., Murphy, D.J., Reid, I.M., Holdsworth, D.A., Vincent, R.A., 2004. First polar mesosphere summer echoes observed at Davis, Antarctica (68.6S). Geophysical Research Letters 31, L16111.

Morrison, R.J., Murphy, D., Klekociuk, A., Holdsworth, D.A., 2007. First complete season of PMSE observations above Davis, Antarctica, and their relation to winds and temperatures . Geophysical Research Letters 34, L05805.1–L05805.5.

Offermann, D., 1985. The Energy Budget Campaign 1980. Journal of Atmospheric and Terrestrial Physics 47, 1–26.

Ogawa, T., Nozawa, S., Tsutumi, M., Arnold, N.F., Nishitani, N., Sato, N., Yukimatu, A.S., 2004. Arctic and Antarctic polar mesosphere summer echoes observed with oblique incidence HF radars: analysis using simultaneous MF and VHF radar data. Annales Geophysicae 22, 4049–4059.

Ogunjobi, O., Sivakumar, V., Mbatha, N., 2014. A Case Study of Energy Deposition and Absorption by Magnetic Cloud Electrons and Protons over the High Latitude stations: Effects on the Mesosphere and Lower Thermosphere . Terrestrial, Atmospheric and Oceanic Sciences 25, In press.

Palmer, J.R., Rishbeth, H., Jones, G.O.L., S., W.P.J., 1996. A statistical study of polar mesosphere summer echoes observed by EISCAT. Journal of Atmospheric and Solar–Terrestrial Physics 58, 307–315.

Rapp, M., Lübken, F.J., 2004. Polar mesosphere summer echoes (PMSE): review of observations and current understanding. Atmospheric Chemistry and Physics Discussions 4, 4777–4876.

Richardson, I.G., Cliver, E.W., Cane, H.V., 2001. Sources of geomagnetic storms for solar minimum and maximum conditions during 1972-2000. Geophysical Research Letters 28, 2569–2572.

Röttger, J., 1994. Polar mesosphere summer echoes: Dynamics and aeronomy of the mesosphere. Advances in Space Research 14, (9)123–(9)137.

Schunk, R.W., Nagy, A.F., 2000. Ionospheres – Physics, Plasma Physics, and Chemistry. Cambridge University Press, Campbridge.

Smirnova, M., Belova, E., Kirkwood, S., Mitchell, N., 2010. Polar mesosphere summer echoes with ESRAD, Kiruna, Sweden: Variations and trends over 1997–2008. Journal of Atmospheric and Solar-Terrestrial Physics 72, 435–447.

Wilson, A., Stoker, P., 2002. Imaging riometer observations on energetic electron precipitation at SANAE IV, Antarctica. Journal of Geophysical Research 107, 1268.

Wu, C.C., Gopalswamy, N., Lepping, R.P., Yashiro, S., 2013. Characteristics of magnetic clouds and interplanetary coronal mass ejections which cause intense geomagnetic storms. Terrestrial, Atmospheric and Oceanic Sciences 24, 233–241.

Yukimatu, A.S., Tsutumi, M., 2002. A superDARN meteor wind measurement: Raw time series analysis method and its application to mesopause region dynamics. Geophysical Research Letters 29, 1981.

Yukimatu, A.S., Tsutumi, M., 2003. Correction to "A new SuperDARN meteor wind measurement: Raw time series analysis method and its application to mesopause region dynamics" by Akira Sessai Yukimatu and Masaki Tsutsumi. Geophysical Research Letters 30, 1026.

Zeller, O., Hoffmann, P., Bremer, J., Singer, W., 2009. Mesosphere summer echoes, temperature, and meridional wind variations at mid and polar latitudes. Journal of Atmospheric and Solar-Terrestrial Physics 71, 931–942.

Zhang, Y., Paxton, L.J., Kil, H., 2013. Multi-periodic auroral and thermospheric variations in 2006. Terrestrial, Atmospheric and Oceanic Sciences 24, 207–212.

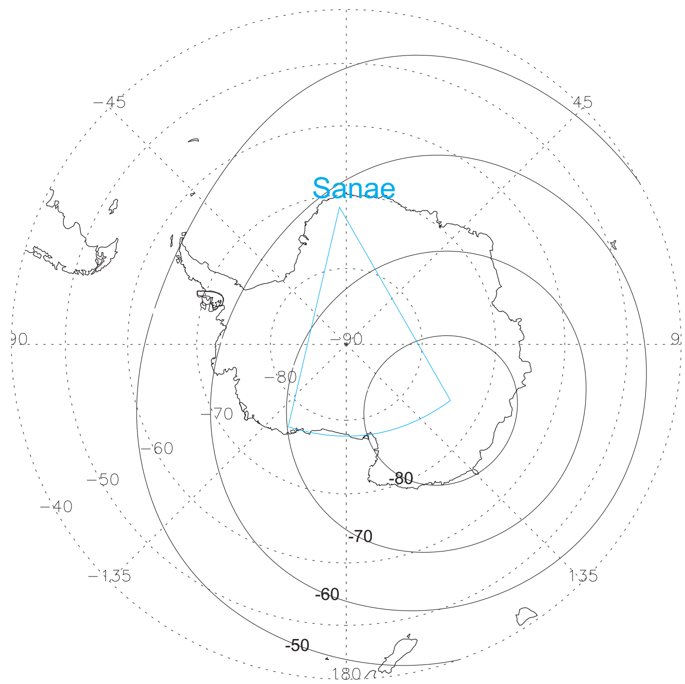

Figure 1: Map showing the SANAE radar field of view (blue line) projected on a geographic (dash lines) and geomagnetic (solid lines) coordinates.

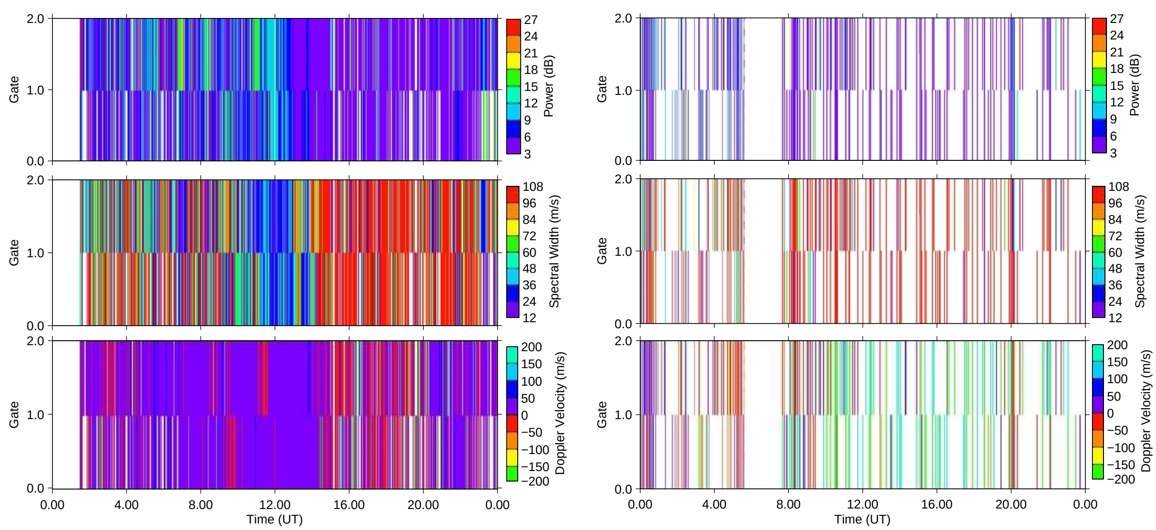

Figure 2: SuperDARN SANAE IV scatter plot of backscatter power, spectral width and Doppler velocity. Beam 12 near range gates on 21 December 2005 (Left panel) and 21 April 2005 (Right).

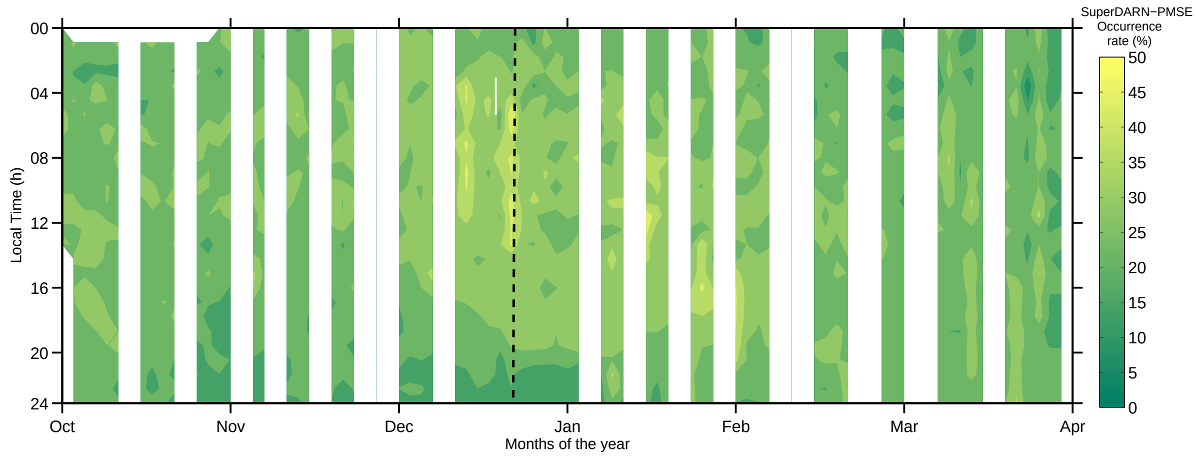

Figure 3: SuperDARN–PMSE occurrence probability rate at SANAE IV during Oct 2005–April 2006 summer season. The vertical dash line indicates December solstice.

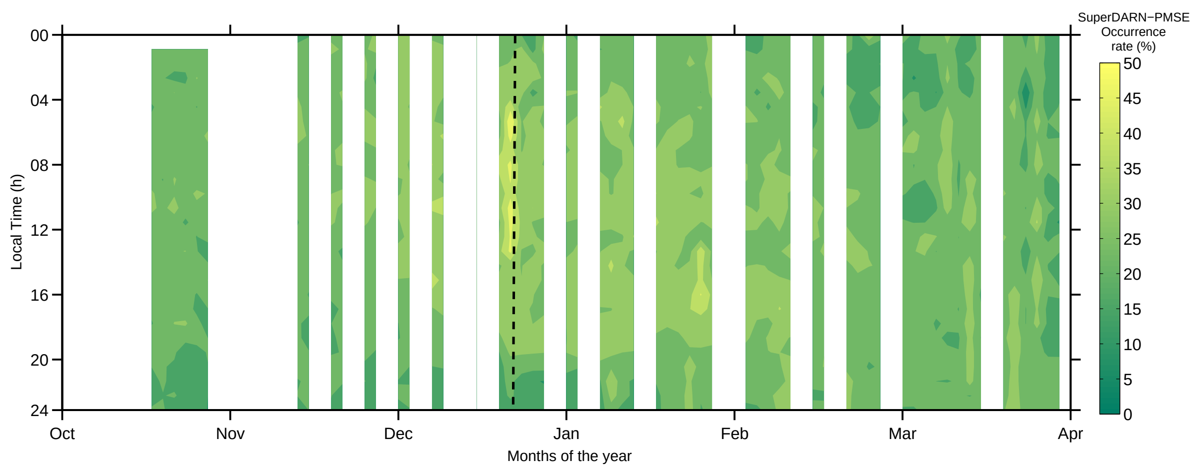

Figure 4: Same as Figure 3 but for Oct 2006–April 2007 summer season.

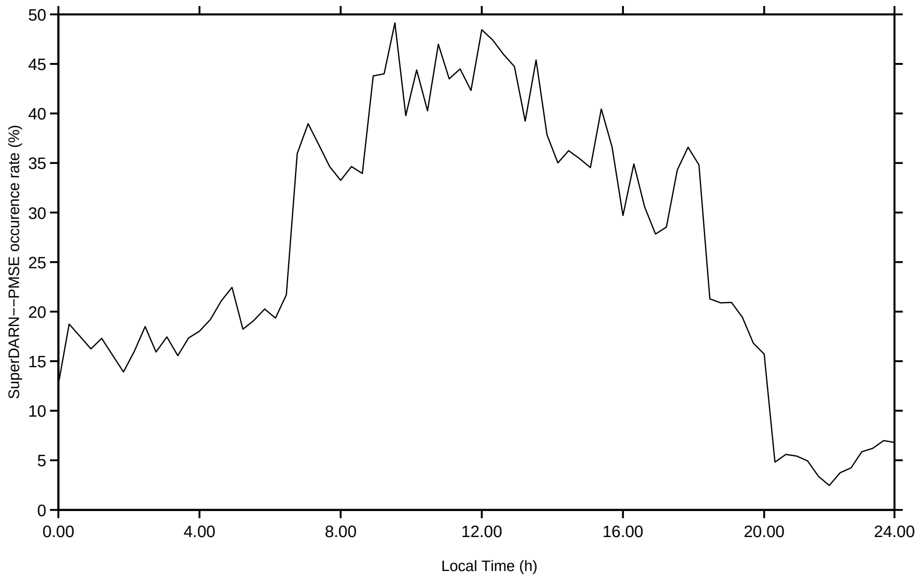

Figure 5: Mean diurnal SuperDARN–PMSE occurrence over SANAE IV for the year 2005/2006 and year 2006/2007 summers.

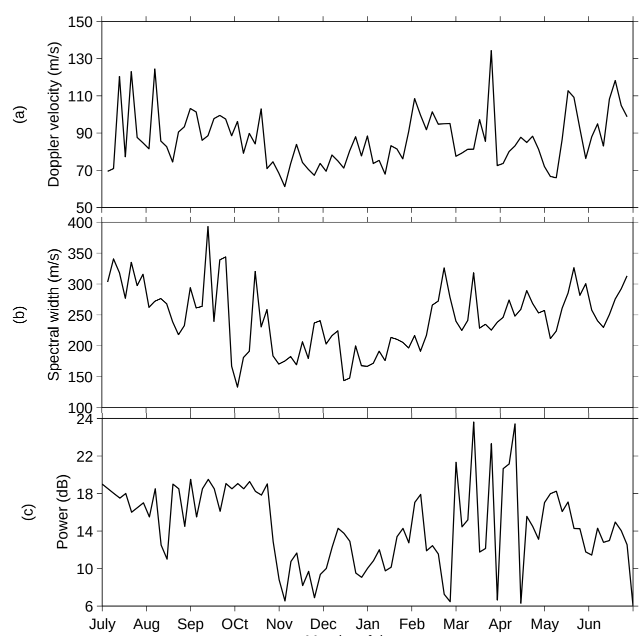

Figure 6: Monthly mean variation of SuperDARN SANAE IV radar Doppler velocity (top panel), spectral width (middle) and power (bottom) from the year 2005 to 2007.

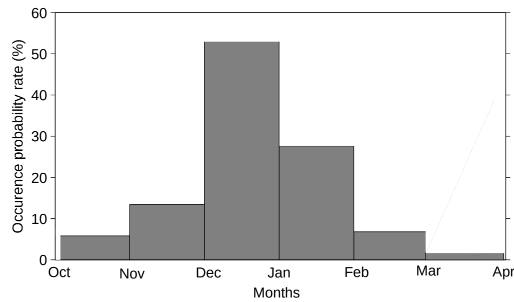

Figure 7: Histogram represents the SuperDARN–PMSE occurrence probability distribution with initial conditions during summer months.

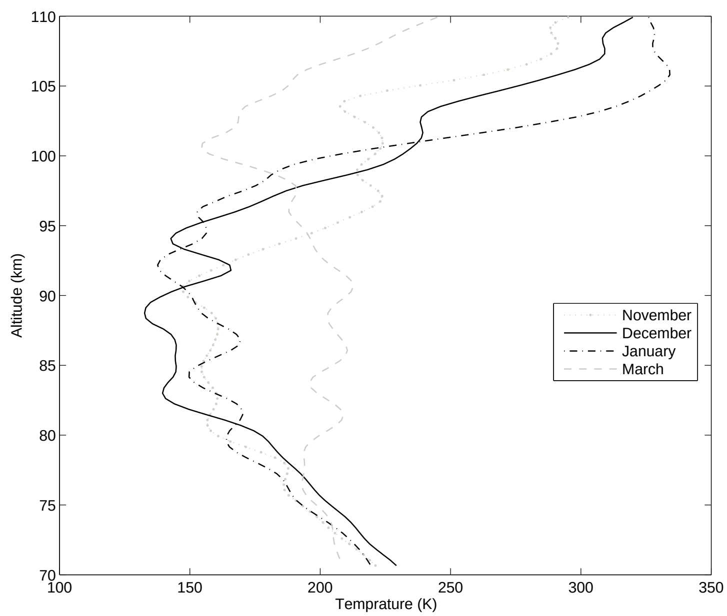

Figure 8: SABER mean temperature profile for November (dot–circle line), December (thick line), January (dash–dot line) and March (dash line) SuperDARN–PMSE season in the vicinity of SANAE IV.

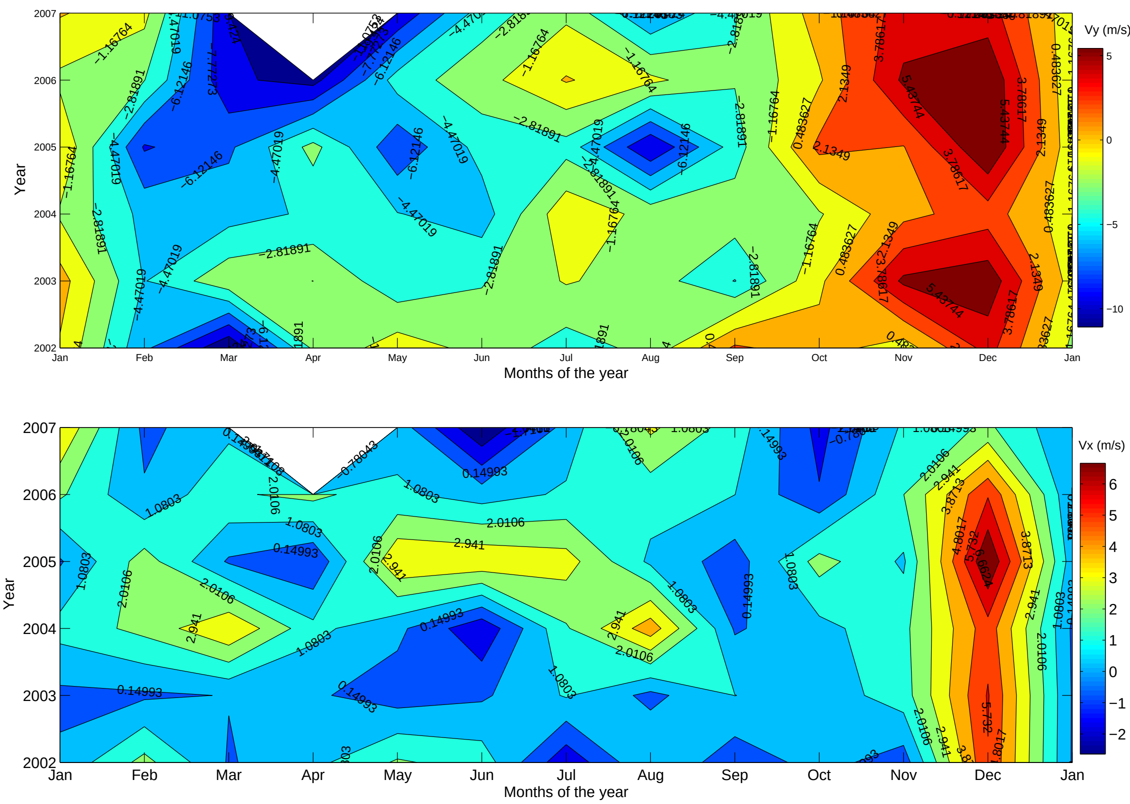

Figure 9: Monthly–variations of meridional (top) and zonal (bottom) mean winds from the year 2002 to 2007.